Eur Respir J, 1993, 6, 772–784
Printed in UK - all rights reserved

European Respiratory Journal
ISSN 0903 - 1936

Respiratory mechanics studied by forced oscillations during artificial ventilation

R. Peslin*, J. Felicio da Silva*, C. Duvivier*, F. Chabot**

Respiratory mechanics studied by forced oscillations during artificial ventilation. R. Peslin, J. Felicio da Silva, C. Duvivier, F. Chabot. ©ERS Journals Ltd.

ABSTRACT: Potential advantages of the forced oscillation technique over other methods for monitoring total respiratory mechanics during artificial ventilation are that it does not require patient relaxation, and that additional information may be derived from the frequency dependence of the real (Re) and imaginary (Im) parts of respiratory impedance. We wanted to assess feasibility and usefulness of the forced oscillation technique in this setting and therefore used the approach in 17 intubated patients, mechanically ventilated for acute respiratory failure.

Sinusoidal pressure oscillations at 5, 10 and 20 Hz were applied at the airway opening, using a specially devised loudspeaker-type generator placed in parallel with the ventilator. Real and imaginary parts were corrected for the flow-dependent impedance of the endotracheal tube; they usually exhibited large variations during the respiratory cycle, and were computed separately for the inspiratory and expiratory phases.

In many instances the real part was larger during inspiration, probably due to the larger respiratory flow, and decreased with increasing frequency. The imaginary part of respiratory impedance usually increased with increasing frequency during expiration, as expected for a predominately elastic system, but often varied little, or even decreased, with increasing frequency during inspiration. In most patients, the data were inconsistent with the usual resistance-inertance-compliance model. A much better fit was obtained with a model featuring central airways and a peripheral pathway in parallel with bronchial compliance. The results obtained with the latter model suggest that dynamic airway compression occurred during passive expiration in a number of patients.

We conclude that the use of forced oscillation is relatively easy to implement during mechanical ventilation, that it allows the study of respiratory mechanics at various points in the respiratory cycle, and may help in detecting expiratory flow limitation.

Eur Respir J., 1993, 6, 772–784.

* Unité 14 de Physiopathologie Respiratoire, Institut Natiónal de la Santé et de la Recherche Médicale, Université de Nancy I, Nancy, France. ** Service des Maladies Respiratoires et Réanimation Respiratoire, CHU Nancy-Brabois, Vandoeuvre-les-Nancy, France.

Correspondence: R. Peslin
Unité 14 INSERM de Physio-Pathologie Respiratoire
C.O. n° 10
54511 Vandoeuvre-les-Nancy
France

Keywords: Acute respiratory failure
mechanical ventilation
modelling
respiratory impedance

Received: September 7 1992
Accepted after revision March 10 1993

A number of studies have recently been devoted to respiratory mechanics during artificial ventilation. In particular, two types of methods have been used: interruption methods, as proposed by the Montreal group [1–5], and fitting of a model to the respiratory pressure-flow relationship by multiple linear regression (MLR) [6–9]. When these methods are applied to the total respiratory system, it is required that the subjects be passive, so that tracheal pressure actually represents the total pressure driving the respiratory system. Although the MLR method has been successfully used to obtain total elastance and resistance in conscious non-paralysed patients [8], this requirement limits the applicability of these methods. A potentially interesting alternative is the forced oscillation technique [10], which does not necessitate respiratory muscle relaxation, because the frequency of the oscillations may be much higher than that of breathing. One may also hope that the enlarged frequency range will provide additional information on respiratory mechanics.

The objective of this study was to evaluate the feasibility and usefulness of studying respiratory mechanics by the forced oscillation technique in artificially ventilated patients with acute respiratory failure.

Methods

Forced oscillation measurements

The subject was connected in parallel to the ventilator and to a specially devised pressure generator. The latter had to meet a number of requirements:

1) it should not interfere with the mechanical ventilation; this implied that the generator had a high impedance at low-frequency;

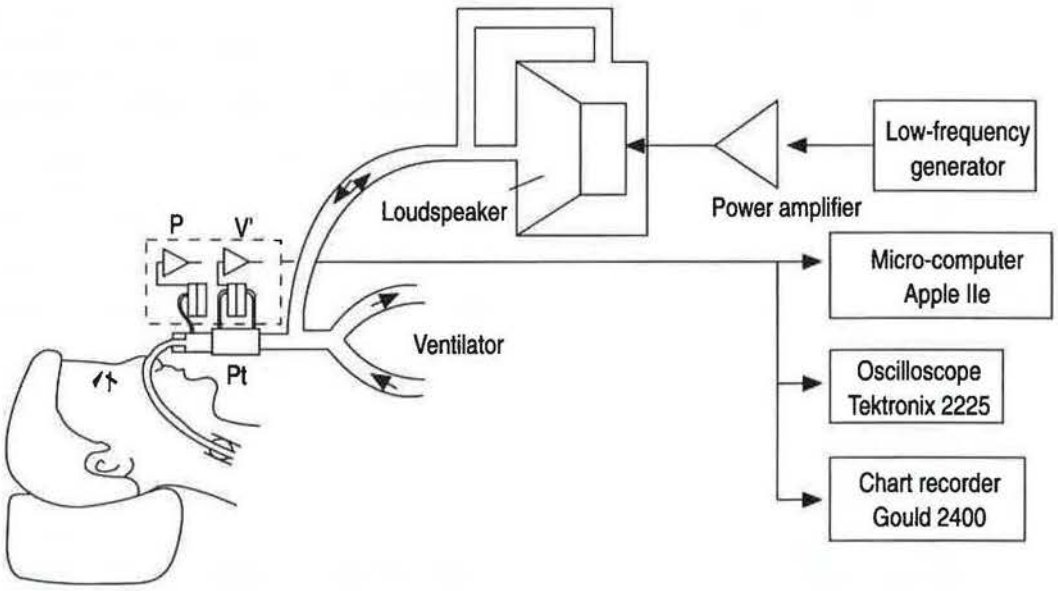

Fig. 1. – Experimental set-up. Pt: pneumotachograph; P: pressure; V': flow.

2) it should stand the large pressure changes (up to 60 hPa) and fast pressure transients developed by the ventilator;
3) it should generate pressure swings in the frequency range of 5–30 Hz, with a nearly constant amplitude of about 2 hPa peak-to-peak during the whole ventilatory cycle;
4) it should be acceptably small and light, for use in an intensive care unit.

This was achieved by using a small loudspeaker (Audax HD 13 B 25, 30 W) enclosed in a 2.5 *l* box and shunted by a tube (fig. 1). The latter offered little impedance to the low-frequency pressure variations applied by the ventilator [11]. Owing to the shunt, these pressure components were almost the same on both sides of the loudspeaker membrane, even during the fast transition from inspiration to expiration. On the other hand, the tube had a comparatively large impedance for the high frequency signals generated by the loudspeaker itself, so that those signals were little attenuated. The dimensions of the tube which best met the requirements (length 300 cm, ID 1.2 cm) were found by numerical simulation, and the adequacy of the system was tested on mechanical analogues connected to a ventilator. The generator, including the connecting tubes, had an overall compliance of about 1.6 ml·hPa^{-1} and, therefore, minimally influenced the flow delivered to the subject by the ventilator. The loudspeaker was supplied with sinusoidal signals, provided by a low-frequency generator through a power amplifier. A sinusoidal input was preferred to the frequently used composite signals, in order to have the best possible signal/noise ratio, and because the measured system included non-linear components [12].

Airway flow (V') was measured with a Fleisch No. 1 pneumotachograph, placed close to the endotracheal tube (ET), and connected to a Honeywell pressure transducer (type 176 PC ±35 hPa). The common mode rejection ratio of the flow channel, which is a critical factor when large impedances are to be measured [13], was of 60 dB at 30 Hz. Airway opening pressure (Paw_o) was sampled with a similar transducer, matched to the first within 1% of amplitude and 2° of phase, up to 30 Hz.

At each frequency, Paw_o and V' were sampled for 200 consecutive oscillation cycles, and were digitized by an Apple 2e microcomputer system, with a sampling rate of 8 points per cycle. The real (Re) and imaginary (Im) parts of the impedance (Zrs) were derived on a cycle per cycle basis, from the Fourier coefficients of the pressure and flow signals at the excitation frequency. The data were corrected for the time constant of the Fleisch pneumotachograph (2.1 ms) [14]. In this study, Paw_o was measured at the proximal end of the ET, rather than at the distal end, as suggested by others [15, 16], because the patients were already intubated when the examination was performed, and we wanted to be as noninvasive as possible. The measured impedance, therefore, included that of the ET, which had to be corrected for. This was performed using the respiratory component of the measured flow and correction factors, obtained as described in the Appendix.

Subjects and protocol

The study was conducted in 17 patients, admitted to the intensive care for acute respiratory failure. Their biometric characteristics and diagnosis are given in table 1. Most had a history of chronic obstructive or restrictive respiratory disease, and their decompensation had often been triggered by a respiratory infection. They were intubated with Portex ET tubes (ID 7.0–8.5 mm). They were in a stable clinical condition at the time of examination, and were neither sedated nor paralysed. The measurements were made with three different modes of controlled artificial ventilation:

Table 1. – Patients' biometric characteristics and diagnosis

Pt	Sex	Age yrs	Diagnosis
GH	M	76	COPD, acute bronchitis
MM	F	79	Bronchopneumonia
LS	M	71	COPD
ARG	M	79	COPD, acute bronchitis
AC	M	60	COPD, acute bronchitis
AD	M	61	COPD, legionellosis
JK	M	65	TB seq., COPD, viral infection
EM	M	54	COPD, bronchopneumonia
MS	F	66	Obesity, acute bronchitis
CM	F	59	TB seq., COPD, acute bronchitis
JG	M	42	COPD, Kyphoscoliosis, acute bronchitis
MTG	F	67	Kyphoscoliosis
OP	F	60	COPD, emphysema
KJ	M	71	Acute bronchitis
PG	F	68	ARF post cardiac surgery
FP	M	78	TB seq., COPD
PV	M	76	Pleuro-pneumonia

Pt: patients; COPD: chronic obstructive pulmonary disease; TB seq.: sequelae of pulmonary tuberculosis; ARF: acute respiratory failure.

1) Mode 1: without end-inspiratory pause (EIP) and without positive end-expiratory pressure (PEEP).
2) Mode 2: with an EIP of 0.4–1 s, without PEEP; this mode has been advocated for improving gas distribution in the lung [17].
3) Mode 3: with an EIP as above, and with a PEEP of 5–10 hPa; the expected effect of the PEEP was to improve gas distribution and to decrease expiratory flow limitation [3, 8, 18].

Ventilation was almost the same in the three ventilatory modes. In each mode, total respiratory impedance was measured consecutively, at frequencies of 5, 10 and 20 Hz. With the pressure generator used in this study, a sufficiently high signal/noise ratio could not be obtained below 5 Hz.

Data analysis

Large variations of impedance were usually observed during the respiratory cycle, as exemplified in figure 2a: Re(Zrs) exhibited a strong flow dependence, being much lower during the end-inspiratory pause than during flow. Im(Zrs) was much less flow dependent, but often varied according to the flow direction. In view of these

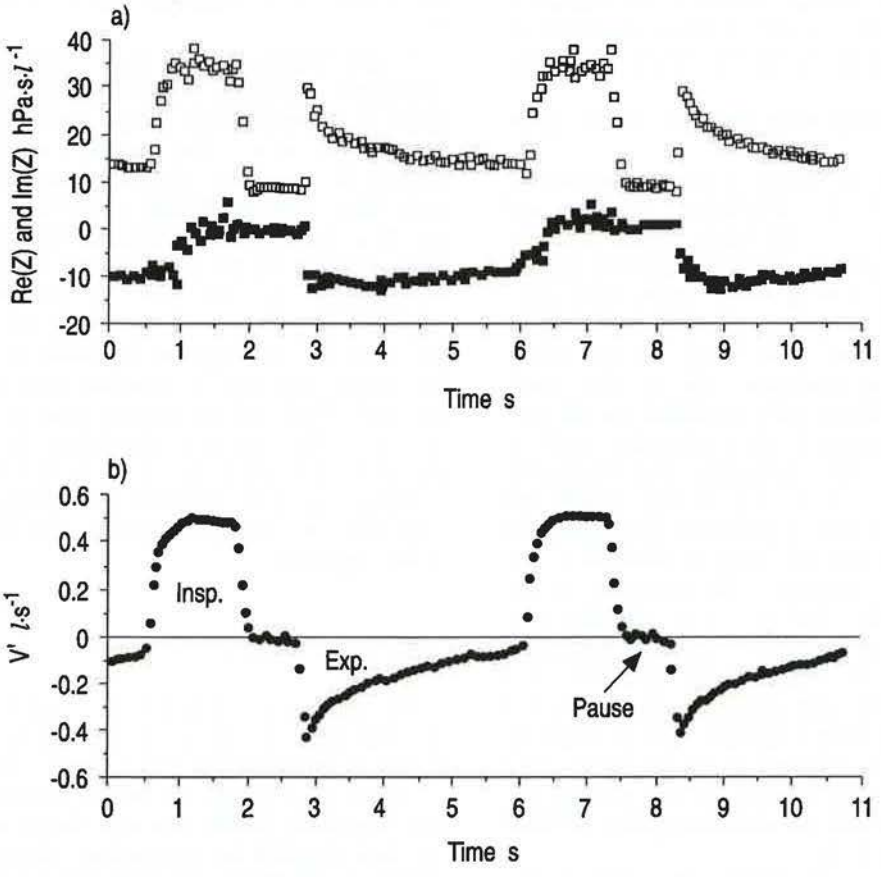

Fig. 2. – a) Variations of the real (Re(Z)) and imaginary (Im(Z)) parts of impedance during the respiratory cycle in one of the patients (excitation frequency of 20 Hz, ventilatory mode 2, which includes an end-inspiratory pause of 0.4–1 s, but no positive end-expiratory pressure (PEEP). ❑ : Re(Zrs); ■ : Im(Zrs). b) The respiratory component of the flow signal. V': airway flow; Insp: inspiration; Exp: expiration. The data have been corrected for the impedance of the endotracheal tube.

variations, mean values of Re(Zrs) and Im(Zrs) were obtained separately for the different phases of the respiratory cycle. These phases were identified using the respiratory component of the flow signal, obtained by averaging instantaneous flow during the oscillation cycle (fig. 2b); inspiration was defined by a flow above 0.05 $l \cdot s^{-1}$, the end-inspiratory pause by a flow between 0.05 and -0.05 $l \cdot s^{-1}$, and expiration by a flow below -0.05 $l \cdot s^{-1}$. For a given phase, the data from all the recorded respiratory cycles (2 to 11 depending on the oscillation and breathing frequencies) were averaged.

The data were systematically analysed with the four models shown in figure 3. Model 1 was the usual resistance-inertance-compliance model; however, to account for the large variations of Zrs along the cycle, the resistance was allowed to take different values for the different respiratory phases: it is, therefore, a 4-coefficient model for ventilatory mode 1, and a 5-coefficient model for the other ventilatory modes. Models 2 and 3 incorporated the type of mechanical non-homogeneity described by MEAD [19], and related to bronchial wall compliance (Cb): in model 2, Cb is in parallel with the whole airway, lung and chest wall, whilst in model 3, Cb is located between a central and a peripheral airway segment. As in model 1, different resistances have been allowed for the different respiratory phases. Finally, model 4 represented the type of mechanical non-homogeneity described by OTIS *et al.* [20], and featured two compartments in parallel with different mechanical time constants. Here again, the resistances were allowed to vary with the respiratory phase. The models were fitted to the data using a simple algorithm [21] to minimize the root-mean-square difference (RMSD) between the observed (index o) and model (index m) impedances:

$$RMSD = [n^{-1} \cdot \sum_{1}^{n} (Re_o - Re_m)^2 + (Im_o - Im_m)^2]^{1/2}$$

where n is the number of impedance data. The analysis was not performed separately for the different respiratory phases, but globally, using all the available data. Then n=6 with ventilatory mode 1, and n=9 with the other modes (3 frequencies times 2 or 3 respiratory phases). The residual RMSD is an expression of the quality of the fit between the model and the data.

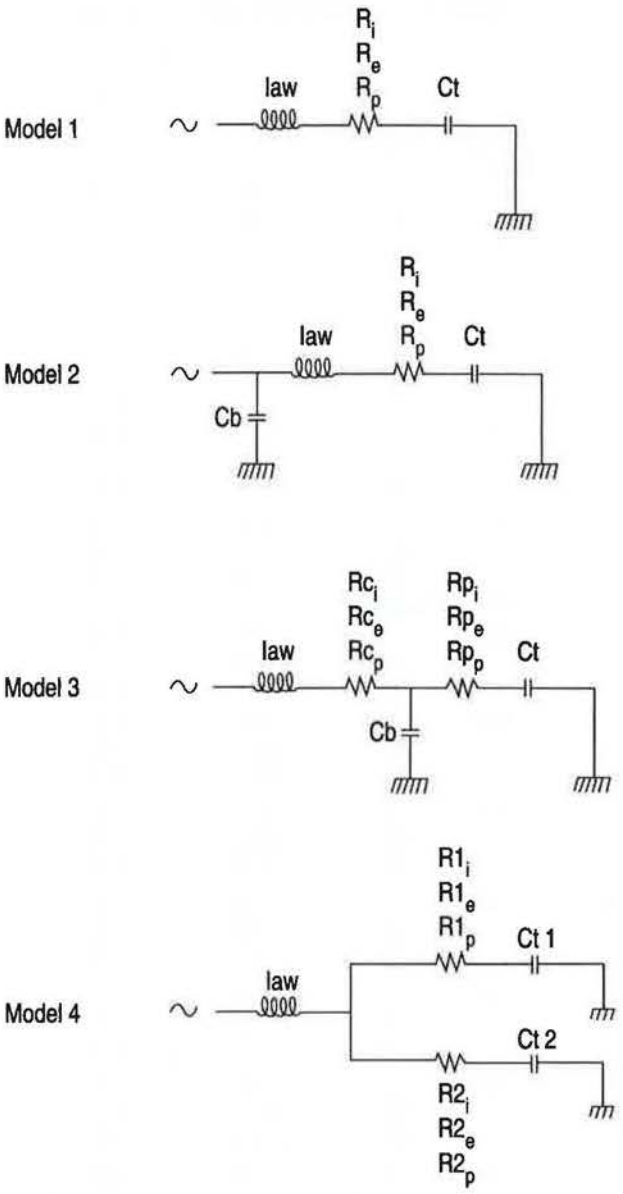

Fig. 3. – Models used to interpret the impedance data. Iaw: airway inertance; Ct: tissue compliance; Cb: bronchial wall compliance; R, Rc, Rp: total respiratory, central and peripheral resistance. Indices i, e and p refer to inspiration, expiration and end-inspiratory pause; indices 1 and 2 refer to compartments in parallel.

Results

Types of impedance curves

Individual data obtained with ventilatory mode 2 are presented in table 2. Two types of impedance data were observed. Representative examples are shown in figure 4.

In type 1 subjects, Re(Zrs) showed little frequency dependence. Im(Zrs) increased with increasing frequency, whatever the respiratory phase, as one expects in a system exhibiting elasticity and inertia.

Type 2 subjects exhibited more frequency dependence of Re(Zrs), and had a very special pattern for the reactance: during the pause Im(Zrs) was small, and increased with frequency; during inspiration, it did not vary much with frequency (as in the example shown in figure 4b), or even decreased with increasing frequency; finally, during expiration, Im(Zrs) increased with frequency, but was much more negative than during the other phases.

With ventilatory mode 1, type 1 and type 2 data were observed in 5 and 12 subjects, respectively. The addition of an end-inspiratory pause did not change that grouping. When a PEEP was added, the real part of impedance was usually lower, and the occurrence of type 2 data was less frequent.

Table 2. – Impedance data in ventilatory mode 2*

Pt	Freq Hz	Re(Zrs)			Im(Zrs)		
		Insp	Exp	Pause	Insp	Exp	Pause
Type 1 subjects							
AD	5	20.22	13.97	3.65	-0.64	-0.65	-0.33
	10	22.88	13.68	3.20	-1.47	-0.97	-0.13
	20	20.95	13.94	2.82	2.62	0.86	1.09
JG	5	4.04	3.58	2.03	-1.37	-1.71	-1.92
	10	3.40	3.41	1.81	-0.28	-0.18	-0.66
	20	3.73	3.16	1.54	0.71	0.27	0.02
MTG	5	10.82	14.91	4.25	-2.74	-5.76	-2.85
	10	11.17	14.27	3.58	-1.87	-3.84	-1.68
	20	10.82	14.93	3.79	-2.17	-7.05	-1.28
PG	5	10.20	4.54	2.24	-1.95	-1.48	-2.44
	10	8.58	4.31	1.45	-1.72	-0.82	-1.14
	20	8.31	4.32	1.84	-0.01	0.27	0.34
PV	5	4.74	2.03	2.08	-0.68	-1.24	-1.01
	10	4.35	1.96	1.72	-0.88	-0.60	-0.82
	20	5.19	1.54	1.20	-0.02	-0.51	-0.51
Type 2 subjects							
GH	5	11.56	12.42	3.96	-0.81	-58.63	-0.30
	10	9.44	7.13	2.82	-3.24	-32.21	-0.63
	20	8.64	4.90	2.83	-4.01	-21.1	-0.88
MM	5	13.04	13.81	3.77	-3.55	-19.96	-1.69
	10	10.67	5.92	3.60	-4.05	-15.06	-1.54
	20	9.72	3.25	3.26	-4.29	-7.12	-0.51
LS	5	9.67	13.89	3.85	-0.94	-20.66	0.30
	10	10.69	7.73	3.31	-2.14	-19.01	0.05
	20	8.34	4.61	2.95	-2.03	-8.61	0.78
ARG	5	12.38	9.82	3.42	-4.19	-12.06	-2.05
	10	6.52	3.51	2.27	-4.92	-6.86	-1.99
	20	5.19	2.09	1.88	-4.55	-4.75	-1.82
AC	5	36.56	32.77	8.29	-3.21	-25.33	-1.66
	10	35.65	20.95	7.16	-3.10	-20.85	-1.06
	20	32.77	14.73	8.21	-0.75	-11.08	-0.84
JK	5	17.05	14.55	4.58	-3.21	-24.16	-1.86
	10	14.21	8.11	4.26	-3.83	-14.61	-1.04
	20	11.83	5.91	4.06	-3.55	-6.45	-0.41
EM	5	11.73	14.64	3.32	-1.28	-12.65	-0.42
	10	10.66	9.52	2.98	-2.70	-9.45	-0.34
	20	9.06	5.21	3.23	-2.71	-4.85	0.81
MS	5	28.18	13.78	2.93	0.14	-7.46	-0.65
	10	24.79	15.22	1.66	-0.98	-5.77	-0.51
	20	18.08	7.58	1.87	-11.25	-4.69	0.63
CM	5	16.26	44.97	6.42	-3.98	-61.61	-2.81
	10	15.92	24.82	5.34	-4.87	-48.17	-2.26
	20	13.27	15.91	5.80	-6.85	-27.14	-1.46
KJ	5	7.82	5.01	2.61	-0.97	-9.38	-0.86
	10	6.98	3.62	1.84	-1.40	-8.12	-0.57
	20	6.15	2.49	3.03	-3.94	-3.26	0.32
FP	5	5.91	5.19	2.37	-1.00	-2.30	-1.37
	10	7.77	7.95	2.32	-1.05	-5.78	-0.60
	20	7.14	3.48	2.07	-1.55	-1.19	-0.73
OP	5	21.79	13.85	6.25	-2.41	-46.95	-3.72
	10	20.15	7.01	5.49	-1.47	-25.74	-2.57
	20	24.38	4.60	3.91	-17.53	-12.83	-1.72

*: Mode 2 ventilation includes an end-inspiratory pause of 0.4–1 s, but no PEEP. Re(Zrs), Im(Zrs): real and imaginary parts of total respiratory impedance ($hPa \cdot l^{-1} \cdot s$).; Freq: frequency; Insp: inspiration; Exp: expiration; PEEP: positive end-expiratory pressure; Pt: patient.

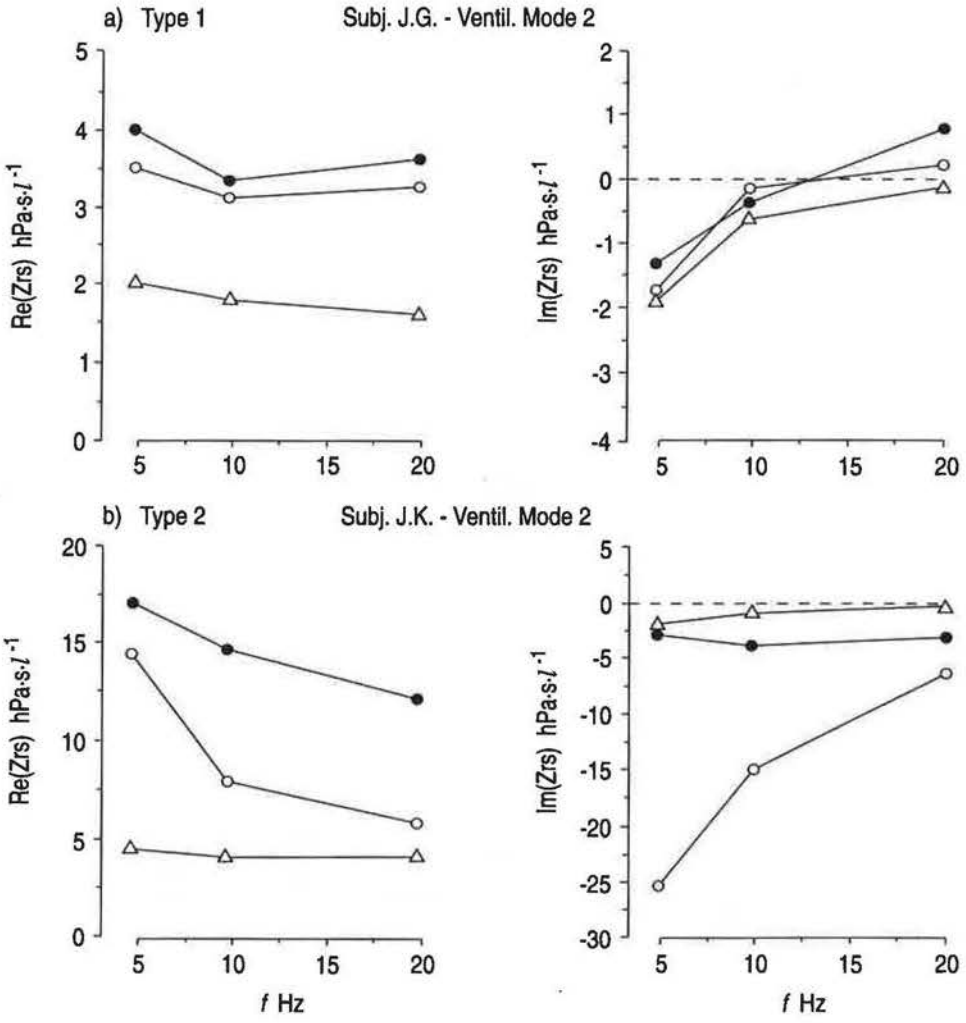

Fig. 4. – Examples of the two types of impedance data. Re(Zrs) and IM(Zrs): real and imaginary parts of impedance. —●—: inspiration; —○—: expiration; —Δ—: end-inspiratory pause. Mode 2: see legend to figure 2.

Relationship to patient diagnosis

No clear relationship was present between the type of impedance data and the patient's diagnosis. Type 2 curves were seen both in patients who had a history of chronic obstructive pulmonary disease (COPD), and in those who had not (MM, MS, KJ). Reciprocally, two of the patients with type 1 data had a history of COPD (AD, JG). Judged from inspiratory Re at 5 Hz in ventilatory mode 2, patients with type 2 data had, in general, more airway obstruction (16.0±8.9 hPa·s·l^{-1}) than patients with type 1 data (10.0±6.5 hPa·s·l^{-1}); one of the latter, however had a Re of 20.2 hPa·s·l^{-1}. Within-breath variations of Re, as characterized by the ratio of the inspiratory and pause values at 5 Hz, were similar in type 1 and type 2 patients (3.38±1.57*vs* 3.78±1.92). In contrast, by definition of the types, type 1 patients had a much lower phase dependence of Im than type 2 patients: at 5 Hz, with ventilatory mode 2, inspiratory and expiratory values differed by 0.7±1.4 hPa·s·l^{-1} in the former group, compared to 23.0±19.6 hPa·s·l^{-1} in the latter group. Phase dependence of Im almost completely disappeared, *i.e.* became smaller than 5 hPa·s·l^{-1}, in all but two patients with ventilatory mode 3.

Model analysis

The residual RMSDs obtained in the 17 patients (ventilatory mode 2) with models 1–3, expressed as percentages of the mean impedance moduli, are shown in figure 5. With type 1 subjects, the data were fairly consistent with model 1, and the fit improved little with models 2 and 3. In the other subjects, the fit was poor or bad with model 1, which can neither account for a frequency dependence of Re(Zrs) nor for variations of Im(Zrs) with the respiratory phase. In most instances, a much better fit was seen with model 2 and/or model 3. This is illustrated in figure 6, which shows a case where model 3 almost perfectly fitted the data. In all instances, the fit obtained with model 4 was slightly less good than with model 3, which had the same number of coefficients.

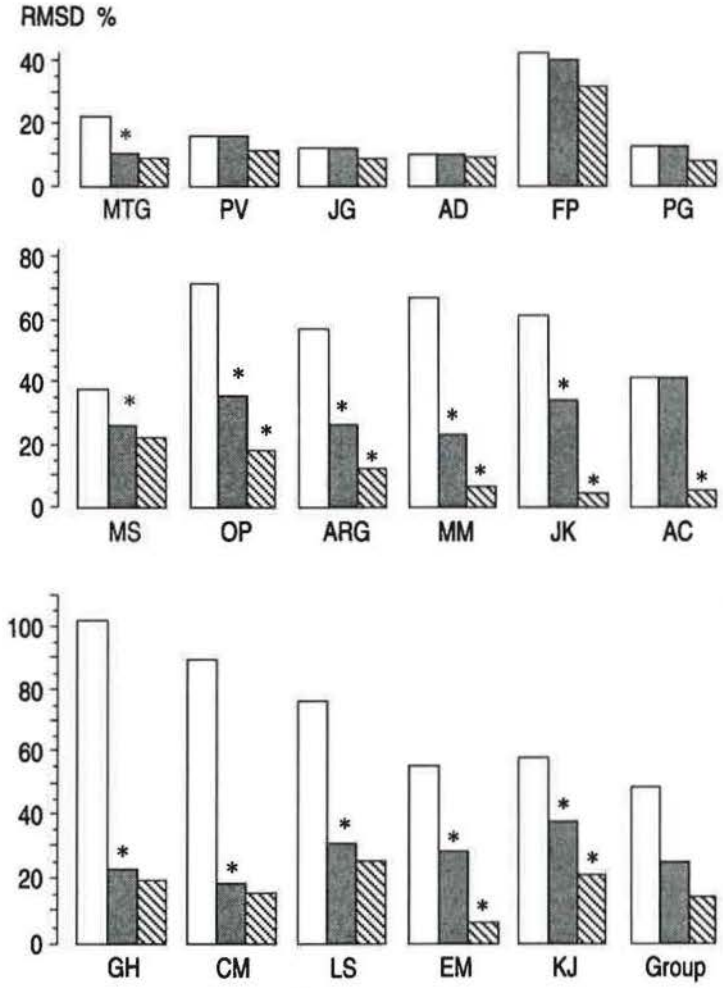

Fig. 5. – Root-mean-square differences (RMSD) between observed and model impedances with models 1–3, expressed as a percentage of the mean impedance moduli (ventilatory mode 2). Values for 17 individual subjects and mean value in the group. Statistically significant differences ($p<0.05$) between models 1 and 2, and between model 2 and 3 are indicated by an asterisk. □: Model 1; ■ : Model 2; ▨ : Model 3.

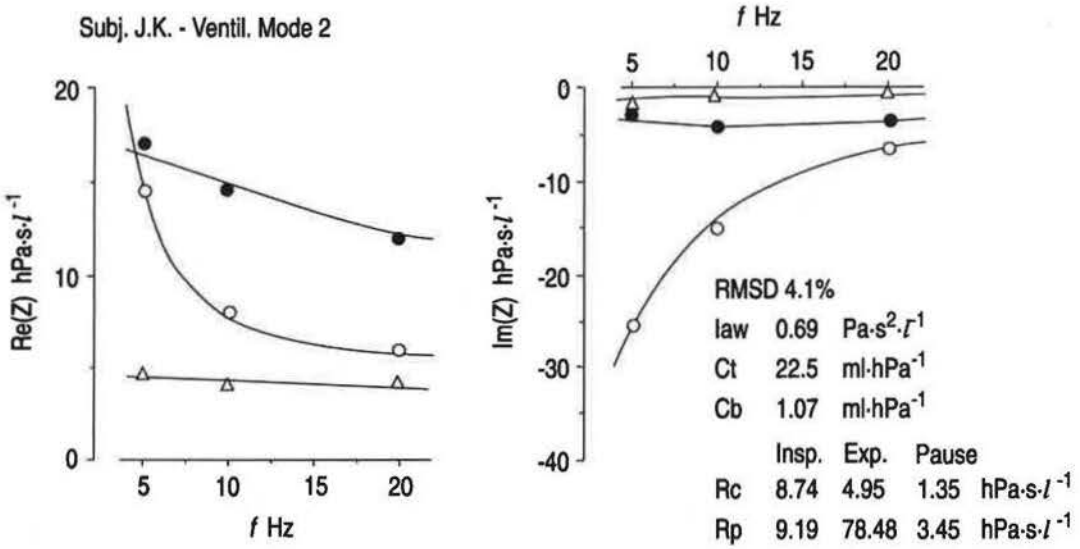

Fig. 6. – Example of best fit between model 3 and type 2 impedance data. ●: inspiration (Insp);○: expiration (Exp.); Δ : end-inspiratory pause. Line indicates best fit of model. For abbreviations see legend to figures 3 and 5. Mode 2: see legend to figure 2.

Table 3. – Coefficients obtained with the selected model for ventilatory mode 2

Pt	Cb	Iaw	$R1_i$	$R1_e$	$R1_p$	Rp_i	Rp_e	Rp_p	Ct
Model 1									
FP		0.00	7.0	5.6	2.2				13.1
PV		0.00	5.0	1.7	1.6				30.1
JG		0.60	3.6	3.3	1.8				17.8
AD		1.29	21.1	13.9	3.1				22.4
PG		0.59	9.1	4.4	1.9				14.1
Model 2									
MTG	0.19	0.49	11.1	16.2	4.0				10.2
MS	0.15	0.00	23.5	12.2	1.8				17.8
GH	0.58	0.50	10.8	171.4	3.1				∞
CM	0.28	1.54	17.4	123.8	6.2				8.1
LS	0.89	1.91	8.5	36.6	3.3				173.2
Model 3									
OP	0.71	0.00	11.9	4.0	0.0	11.9	195.6	6.1	26.0
ARG	1.74	0.00	3.7	1.4	0.0	11.4	26.4	3.6	37.0
MM	1.03	0.00	5.6	1.6	2.2	8.3	48.2	1.2	14.9
JK	1.07	0.69	8.7	4.9	1.3	9.2	78.5	3.5	22.5
AC	0.64	0.82	30.4	11.1	4.2	6.3	53.0	4.0	13.8
EM	1.40	0.36	6.1	4.5	3.1	6.1	27.6	0.1	78.2
KJ	2.56	0.00	4.5	1.7	2.5	4.0	29.3	0.0	55.4

Resistances are in $hPa \cdot s \cdot l^{-1}$, compliances in $ml \cdot hPa^{-1}$ and Iaw in $Pa \cdot s^2 \cdot l^{-1}$. R1: total respiratory resistance for models 1 and 2, central airway resistance for model 3; Cb: compliance of bronchial wall; Iaw: airway inertance; Ct: tissue compliance; Rp: peripheral resistance. Indices i, e and p refer to inspiration, expiration and end-inspiratory pause.

Table 4. – Coefficients obtained with the selected model for ventilatory mode 3

Pt	Cb	Iaw	$R1_i$	$R1_e$	$R1_p$	Rp_i	Rp_e	Rp_p	Ct
Model 1									
FP		0.00	3.6	1.0	1.1				22.2
PV		0.00	3.5	1.1	1.3				25.1
JG		0.70	4.5	2.1	1.5				16.1
AD		1.26	20.9	12.4	2.9				21.2
PG		0.52	6.8	2.7	1.5				10.8
MTG		0.00	9.1	6.6	3.2				9.7
MS		0.00	25.4	12.2	4.7				38.3
AC		0.00	31.1	11.9	6.6				11.8
EM		0.58	8.3	3.7	2.4				32.6
Model 2									
CM	0.16	0.00	23.1	19.7	8.7				10.0
KJ	0.56	0.00	7.7	4.8	1.9				30.6
GH	0.90	1.66	8.7	23.6	3.3				26.6
Model 3									
OP	1.17	0.00	13.8	4.3	2.1	7.4	72.8	3.4	14.2
ARG	2.15	0.00	3.7	0.0	0.0	10.8	13.2	3.8	18.8
MM	1.06	0.63	5.6	1.0	0.6	9.4	17.6	3.3	15.3
JK	0.96	1.22	6.1	6.1	0.0	6.4	5.5	3.7	14.3
LS	0.72	0.56	3.9	0.0	3.0	5.6	10.5	0.0	49.5

For abbreviations see legend to table 3.

In order to select the most acceptable model in each subject, the statistical significance of the differences in RMSD between models was assessed using a standard paired F-test, as proposed by EYLES *et al.* [22]. Model 1 was kept when the fit to both models 2 and 3 was not significantly better, model 3 when it gave a significantly better fit ($p<0.05$) than model 1 and 2, and model 2 in the other instances. The coefficients obtained with the selected model are shown in tables 3 and 4 for ventilatory modes 2 and 3, respectively; the grouping of the patients and the individual results obtained with ventilatory mode 1 were very similar to those found with mode 2 and, therefore, are not reported. The solutions presented in table 3 and 4 were in most instances unique, that is almost identical solutions were found when the parameter estimation was repeated with different starting points.

With ventilatory mode 2, model 1 appeared the most adequate in five patients, four of whom had been

classified as type 1, and models 2 and 3 in five and seven patients, respectively. Airway inertance was in many instances low or undetectable. When present in the model, bronchial compliance averaged 0.94±0.70 ml·hPa^{-1}. Total respiratory compliance was of the order of magnitude usually observed with the forced oscillation technique [23], except in a few instances, where it was unrealistically high. Respiratory resistance, whether total (models 1 and 2), central or peripheral (model 3) was consistently lower during the pauses than during the inspiratory or expiratory phases. With model 1, resistance was often larger during the inspiratory than during the expiratory phase; this was also the case for the central component of airway resistance obtained with model 3. In contrast, the resistance obtained with model 2 and the peripheral resistance of model 3 were consistently larger, sometimes considerably so, during the expiratory than during the inspiratory phase.

With ventilatory mode 3, model 1 was more frequently appropriate than with mode 2 (table 4). The general features of the data were similar to those seen without PEEP, except that the resistance obtained with model 2 and the peripheral resistance of model 3 were no longer systematically larger during the expiratory phase.

As mentioned above, the two-compartment model (model 4) never provided a better fit than model 3, which had the same number of coefficients. The differences, however, were small. In all instances, one of the compartments had a very low compliance, similar to that found for the bronchial walls with models 2 and 3.

Discussion

Feasibility

Respiratory impedance had previously been measured in anaesthetized humans, momentarily disconnected from the ventilator [16, 24]. A first objective of this study was to assess the feasibility of applying the forced oscillation technique during artificial ventilation. It proved comparatively easy to develop a pressure generator, which interfered little with the artificial ventilation, could stand the large pressure changes applied by the ventilator, and provided the required pressure input over the frequency range of interest.

Impedance of endotracheal tubes

As indicated by others, a particular problem when studying respiratory mechanics in intubated patients is the correction of the data for the resistance or impedance of the ET [25–28]. An elegant solution is to measure the pressure at the distal end of the tube, using the lateral catheter of the ETs devised for high frequency ventilation [16]. This is indeed preferable, but could not be done in this study, because the patients were already intubated with standard tubes at the time of the study. It was, therefore, necessary to subtract from the measured impedance that of the ET. Impedances of ETs (Zet) have previously been measured with different amplitudes of the oscillatory flow [28], but without the superimposed low-frequency flow component, as present during artificial ventilation. We, therefore, systematically studied the impedance of the four ETs used in this study, for different oscillatory flows superimposed on a large range of constant flows (Appendix). Using mechanical analogues of the respiratory system, we obtained evidence that the correction was accurate (fig. 7).

Model analysis

While forced oscillation measurements at a single frequency may already be of interest to detect changes in respiratory mechanics [24], the data obtained at several frequencies may be analysed in terms of a model and provide more information on the nature of the changes [29]. In most of our patients Re(Zrs) exhibited a negative frequency dependence, and varied markedly during the respiratory cycle. These features have already been reported in spontaneously breathing patients with chronic obstructive pulmonary disease [23, 30–33]. The most interesting experimental fact, however, was the presence, in many instances, of very large variations of Im(Zrs) during the cycle, with a peculiar frequency dependence during the inspiratory phase: instead of its usual increase with frequency, which is the expected pattern in a system exhibiting elasticity and inertia, Im(Zrs) either varied very little, or decreased, with increasing frequency. Such features have not yet been reported for the total respiratory system, but an absence of frequency dependence of the imaginary part of chest wall impedance was observed by NAGELS *et al.* [32].

None of the features described above can be explained by the usual resistance-inertance-compliance model with constant coefficients. Since even the patients who had little frequency dependence of Re(Zrs) and a normal reactance pattern could present large variations of Re(Zrs) along the cycle, a first step in the modelling was to allow for different resistances in the different respiratory phases. That variant of the usual model appeared satisfactory in five patients for ventilatory modes 1 and 2, and in nine patients when a PEEP was used. It was not the privilege of patients with little airway obstruction since, in some instances, the resistance exceeded 20 hPa·s·l^{-1} during the inspiratory phase. Resistance was usually lowest during the end-inspiratory pause, and larger during inspiration than during expiration. The latter finding probably reflects the flow dependence of this coefficient; indeed, the mean respiratory flow was larger during the inspiratory phase. The inertance coefficient was nil in most instances, which is not surprising since most of inertance of the airway wall (Iaw) is expected to be located in the upper airways which, in this study, was shunted by the ET.

The next step was to account for the negative frequency dependence of Re(Zrs), which may be explained by two mechanisms. The first is the presence of different mechanical time constants in different zones of the lung or of the chest wall; its simplest expression is the two-compartment model proposed by OTIS *et al.* [20].

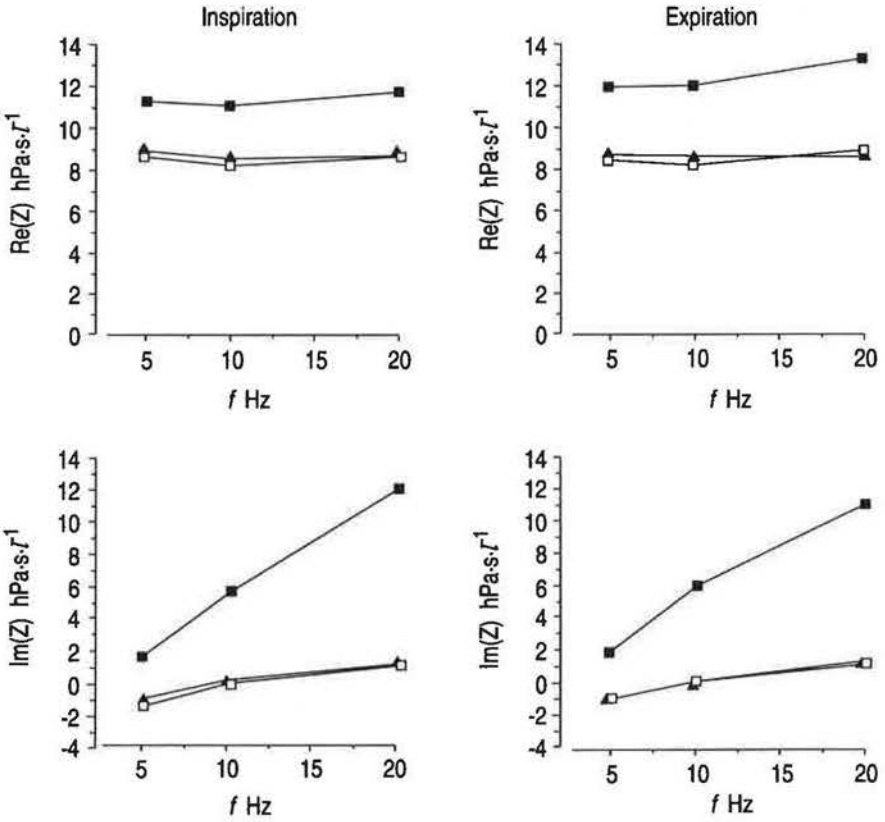

Fig. 7. – Real (Re(Z)) and imaginary (Im(Z)) parts of the impedance of a mechanical analogue. —▲—: analogue alone; —■— : analogue in series with endotracheal tube (7.5 mm Portex); —□—: analogue in series with tube after subtracting the impedance of the tube using the coefficients in table 5 (see Appendix).

The second is the compliance of airway walls, which may constitute a substantial shunt when the impedance of the peripheral lung is large. Models 2 and 3 are simplified representations of the mechanism described by MEAD [19], where, as done by others previously [19, 34], the bronchial compliance has been placed in parallel with both the peripheral lung and the chest wall. Model 3 is slightly more general than model 2, since it does not impose that Cb is in parallel with all of the airways. As expected, model 2 or model 3 were able to mimic the negative frequency dependence of Re(Zrs) present in our subjects. More remarkably, they were also able to account for the large variations of the reactance during the respiratory cycle, and for its unusual frequency dependence in the inspiratory phase. In the light of the coefficients obtained with these models, particularly model 3 with ventilatory mode 2 (table 3), the following interpretation may be given to type 2 impedance data (fig. 6).

Firstly, during the end-inspiratory pause, *i.e.* at zero flow, the peripheral airway resistance is comparatively low, so that the pathway constituted by the airway wall is in parallel with a much lower impedance, and shunts only a very small part of the flow, as is the case in normal subjects [19]. Then, both Re(Zrs) and Im(Zrs) have a normal frequency dependence.

Secondly, during the inspiratory phase, due to the flow dependence of resistance, the peripheral resistance is much higher, so that a larger fraction of the oscillatory flow is shunted by the airway walls; this is responsible for the negative frequency dependence of resistance and the bizarre reactance curve.

Finally, during the expiratory phase, although respiratory flow is less, the peripheral airway resistance is extremely high (almost 80 $hPa \cdot s \cdot l^{-1}$), probably due to dynamic airway compression and, possibly, flow limitation. Then, almost all of the oscillatory flow is shunted by the airway walls, and the reactance largely represents the compliance of these walls. One should point out that Re(Zrs) at 10 and 20 Hz (fig. 6) is much lower than during the inspiratory phase, which may be very misleading if the data are not interpreted with the proper model.

As with model 1, the inertance coefficients found with models 2 and 3 were frequently nil, presumably for the same reason. With ventilatory mode 2, bronchial compliance averaged 0.94 ± 0.70 $ml \cdot hPa^{-1}$. This is low compared to the value of 3.3 $ml \cdot hPa^{-1}$ computed from the change in dead space volume over the vital capacity range [19]. This, again, may be due to the fact that the upper airways are not included in the measurement. Peripheral airway resistance during the expiratory phase (Rp_e) was always larger than during the inspiratory phase, which may be explained by dynamic airway compression. In a number of instances Rp_e was extremely large, suggesting that the subject had reached his or her maximum expiratory flow. In the few subjects in whom model 3 was appropriate in both ventilatory modes 2 and 3, it is also interesting to note that the PEEP always decreased Rp_e. In contrast with the peripheral resistance, the

central component was consistently larger during the inspiratory phase, a finding which, again, points to flow dependence. The latter is also probably responsible for the lower values of peripheral resistance (Rp) and central resistance (Rc) during the end-inspiratory pauses.

Whilst the mechanism described by MEAD [19], and embodied in models 2 and 3, provides a qualitatively and quantitatively acceptable explanation for type 2 impedance data, the model proposed by OTIS *et al.* [20] also fitted these data nicely. However, one of the two compartments identified with that model always had a very low compliance, similar to that found for the bronchial wall with models 2 and 3. If this compartment corresponded to a portion of the lung and chest wall, as postulated in the model of OTIS *et al.* [20], there is no reason why it would have such a low compliance in all of the patients. One would, rather, expect a very large variability among subjects. It is, therefore, more plausible that this compartment actually corresponds to the bronchial wall, and that the results obtained with both types of models point to the same mechanism. That Mead's interpretation was more likely than time constant inequalities of parallel lung units in patients with COPD has already been suggested [23, 31]. Experimental work, however, is still necessary to test this interpretation.

Whilst models 2 and 3 may offer a nice explanation to intriguing data, they cannot be of practical use to analyse impedance curves unless they provide reasonably precise estimates of the coefficients. The confidence intervals (CI) around the latter may be obtained by observing the variability of repeated measurements, or derived analytically from the model, assuming a given level of experimental noise [35, 36]. The approach used in this study is somewhat different: for each model, we first computed impedance values corresponding to a typical set of coefficients. Then, we generated 50 sets of data by adding a random noise to these computed impedance values. We analysed all of these data sets with the usual parameter estimation algorithm, which provided as many sets of coefficients. Finally, we computed the confidence interval of these coefficients at the 95% statistical level (1.64 times their standard deviation). This was done for amplitudes of the noise equal to 10 and to 20% of the mean impedance modulus, which seemed reasonable for our experimental conditions. The initial coefficient set and the CI, expressed as a percentage of the coefficient actual value, are shown in table 5. It may be seen that, whatever the model, the CI are very large for tissue compliance (Ct), which probably explains why some of the Ct values were unrealistic. For Iaw, although we took a larger than observed initial value, CI were also large with models 2 and 3. In contrast, relatively narrow CI were obtained for the resistances, even when they were partitioned into two segments. Finally, the estimates of Cb were remarkably precise.

Practical usefulness

Much more experience should, obviously, be gained before the practical usefulness of the forced oscillation technique for that type of application may be precisely defined. Some conclusions, however, may be drawn from this study. 1) The method is comparatively easy to implement and could be fully automatized to collect data at specified time intervals. 2) The impedance data are frequently inconsistent with the simple resistance-inertance-compliance model, even when allowing for different resistances according to the respiratory phase. A likely explanation for this finding is the compliance of airway walls in parallel with obstructed and/or dynamically compressed airways. More sophisticated models, including airway wall compliance, give a good fit to the data, but provide unreliable values of tissue compliance. 3) A promising feature of the method, compared to other approaches, is its excellent time resolution; it makes it possible, as already shown in other applications [31, 33], to study respiratory mechanics at specific times of the respiratory cycle. Thus, it may be a tool to recognize expiratory flow limitation (or dynamic airway compression), which is certainly useful when adjusting the ventilator settings. This does not necessarily require making measurements at several frequencies and the use of a sophisticated model. Indeed, from our observations, a marked decrease of the reactance during the expiratory phase is very suggestive of flow limitation; one should point out, that the corresponding phasic variations of the real part of impedance at the larger frequencies may be extremely misleading. A practical conclusion of this study is that measurements at a single frequency, as low as it is technically possible, would be useful both to monitor airway obstruction and to detect the occurrence of expiratory flow limitation.

Table 5. – Confidence intervals of the coefficients

		Actual value of coefficient	Confidence intervals %	
			Noise 10%	Noise 20%
Model 1				
	Iaw	2.00	7.7	15.7
	R_i	5.00	3.0	5.4
	R_e	5.00	3.1	6.1
	Ct	40.0	29.4	62.6
Model 2				
	Cb	1.00	2.0	4.6
	Iaw	3.00	64.6	107.1
	R_i	15.0	5.2	9.2
	R_e	100.0	6.7	13.4
	Ct	30.0	>1000	>1000
Model 3				
	Iaw	1.00	47.1	89.7
	Rc_i	5.00	13.1	23.8
	Rc_e	5.00	13.1	27.7
	Cb	1.00	3.0	6.2
	Rp	10.0	8.7	15.6
	Rp_e	100.0	10.7	24.9
	Ct	30.0	814.4	>1000

The confidence intervals are expressed as a percentage of the actual value of the coefficients. For abbreviations see legend to table 3.

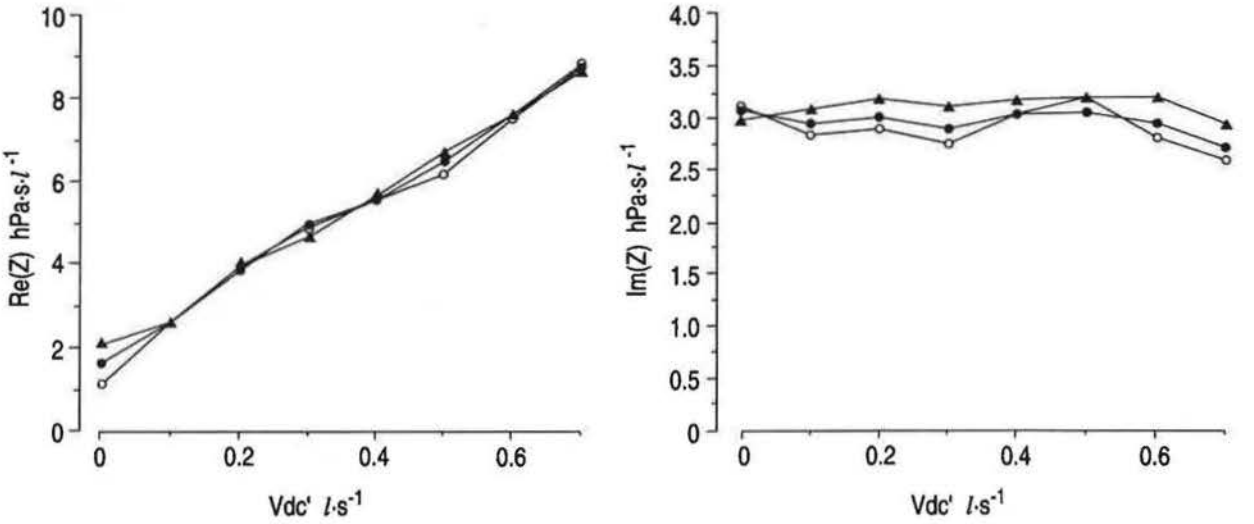

Fig. 8. – Real (Re(Z)) and imaginary (Im(Z)) parts of impedance of an endotracheal tube, ID 7.5 mm, at 5 Hz for different oscillatory flows (Vos') as a function of superimposed constant flow (Vdc') in the inspiratory direction.—○—: Vos' 100 ml·s⁻¹;—●—: Vos' 200 ml·s⁻¹; —▲—: Vos' 300 ml·s⁻¹.

Acknowledgements: The authors are grateful to B. Clement for typing the manuscript and to M.C. Rohrer for the illustration. J. Felicio da Silva was the recipient of a grant from the Coordonaçao de Aperfeiçoamento de Pessoal de Nivel Superior, Ministerio da Educaçao do Brasil.

Appendix

Data correction for the impedance of the endotracheal tube

The impedance of the Portex endotracheal tubes (ID 7.0–7.5 mm, length 32 cm, and ID 8.0–8.5 mm, length 34 cm) was measured using the pressure generator and the transducers described in the method section. The cuffed distal end of the ET was placed in a larger tube, in order to recreate the change in cross-section normally present in the trachea [25]. The pressure difference along the ET was measured from its proximal end, to a point situated in the "trachea" a few centimetres from its distal end; this was done to avoid the measuring artifacts described by CHANG and MORTOLA [26]. The measurements were made at the three frequencies of interest with different amplitudes of the oscillatory flow (Vos'=0.1, 0.2 and 0.3 $l \cdot s^{-1}$) superimposed on constant flows (Vdc') in the inspiratory and expiratory directions ranging from 0–0.7 $l \cdot s^{-1}$.

The results obtained with a 7.5 mm ET, at a frequency of 5 Hz, for inspiratory flows, are shown in figure 8. It may be seen that the real part of impedance (Re(Zet)) did not vary with the amplitude of Vos', except when Vdc' was zero. On the other hand, Re(Zet) increased linearly with Vdc'. The imaginary part of impedance (Im(Zet)) varied a little with Vos', but not consistently, and tended to decrease slightly with increasing Vdc'. Qualitatively similar data were found at the other frequencies, with expiratory flows and with the other tubes. The data were characterized by the following relationships, inspired from Rohrer's equation [37]:

$$Re(Zet) = K1' + K2' \times |Vdc'|$$

$$Im(Zet) = B1 + B2 \times |Vdc'|$$

Coefficients K1', K2', B1 and B2 best fitting the data were obtained by linear regression (K1' and K2' have been used instead of the usual K1 and K2, because the latter generally apply to constant flow conditions). Slightly different values were found according to the frequency and to the direction of Vdc'. For each condition, the values obtained with the three Vos' were averaged and used to correct the impedance data in the intubated patients.

As the impedance of the ET, particularly its imaginary component, may be large compared to that of the patient, a very accurate correction is required. We therefore, tested its adequacy using mechanical analogues of the respiratory system. The analogues included a resistance made of metal screens, a tube and a gas compliance arranged in series. They were connected to a ventilator and to the measuring equipment in the same manner as the patients. An example of the data is shown in figure 7. It may be seen that the corrected impedance is almost identical to the impedance obtained without the ET.

References

1. Bernasconi M, Ploysongsang Y, Gottfried SB, Milic-Emili J, Rossi A. – Respiratory compliance and resistance in mechanically ventilated patients with acute respiratory failure. *Intensive Care Med* 1988; 14: 547–553.
2. Eissa NT, Ranieri VM, Corbeil C, *et al.* – Effects of positive end-expiratory pressure, lung volume, and inspiratory flow on interrupter resistance in patients with adult respiratory distress syndrome. *Am Rev Respir Dis* 1991; 144: 538–543.

3. Gottfried SB, Rossi A, Higgs BD, *et al.* – Non-invasive determination of respiratory system mechanics during mechanical ventilation for acute respiratory failure. *Am Rev Respir Dis* 1985; 131: 414–420.
4. Rossi A, Gottfried SB, Zocchi L, *et al.* – Measurement of static compliance of total respiratory system in patients with acute respiratory failure during mechanical ventilation. *Am Rev Respir Dis* 1985; 131: 672–678.
5. Sly PD, Bates JHT, Milic-Emili J. – Measurement of respiratory mechanics using the Siemens Servo Ventilator 900C. *Pediatr Pulmonol* 1987; 3: 400–405.
6. Benhamou D, Lorino AM, Lorino H, Zerah F, Harf A. – Automated measurement of respiratory mechanics in anaesthetized ventilated patients. *Bull Eur Physiopathol Respir* 1987; 23: 423–428.
7. Nicolai T, Lanteri C, Freezer N, Sly PD. – Non-invasive determination of alveolar pressure during mechanical ventilation. *Eur Respir J* 1991; 4: 1275–1283.
8. Peslin R, Felicio da Silva J, Chabot F, Duvivier C. – Respiratory mechanics studied by multiple linear regression in unsedated ventilated patients. *Eur Respir J* 1992; 5: 871–878.
9. Rousselot JM, Peslin R, Duvivier C. – Evaluation of the multiple linear regression method to monitor respiratory mechanics in ventilated neonates and young children. *Pediatr Pulmonol* 1992; 13: 161–168.
10. DuBois AB, Brody AW, Lewis DH, Burgess BF. – Oscillation mechanics of lungs and chest in man. *J Appl Physiol* 1956; 8: 587–594.
11. Felicio da Silva J. – Monitorage des propriétés mécaniques thoraco-pulmonaires au cours de la ventilation artificielle. Doctoral Thesis, Institut National Polytechnique de Lorraine, 1992.
12. Delavault E, Saumon R. – Fourier analysis of nonlinear fluid systems. *IEEE Trans Biomed Eng* 1982; 29: 215–219.
13. Peslin R, Jardin P, Duvivier C, Begin P. – In-phase rejection requirements for measuring respiratory input impedance. *J Appl Physiol: Respirat Environ Exercise Physiol* 1984; 56: 804–809.
14. Peslin R, Morinet-Lambert J, Duvivier C. – Etude de la réponse en fréquence des pneumotachographes. *Bull Eur Physiopathol Respir* 1972; 8: 1363–1376.
15. Michels A, Landser FJ, Cauberghs M, Van de Woestijne KP. – Measurement of total respiratory impedance *via* endotracheal tube; a model study. *Bull Eur Physiopathol Respir* 1986; 22: 615–620.
16. Navajas D, Farré R, Canet J, Rotger M, Sanchis J. – Respiratory input impedance in anesthetized paralyzed patients. *J Appl Physiol* 1990; 69: 1372–1379.
17. Damman JF, McAslan TC, Maffeo CJ. – Optimal flow pattern for mechanical ventilation of the lungs. The effect of a sine *versus* square wave flow pattern with and without an end-inspiratory pause in patients. *Crit Care Med* 1978; 6: 293–310.
18. Van den Berg B, Stam H, Bogaard JM. – Effects of PEEP on respiratory mechanics in patients with COPD on mechanical ventilation. *Eur Respir J* 1991; 9: 561–567.
19. Mead J. – Contribution of compliance of airways to frequency-dependent behavior of lungs. *J Appl Physiol* 1969; 26: 670–673.
20. Otis AB, McKerrow CB, Bartlett RA, *et al.* – Mechanical factors in distribution of pulmonary ventilation. *J Appl Physiol* 1956; 8: 427–443.
21. Peslin R, Jardin P, Hannhart B. – Modeling of the relationship between volume variations at the mouth and chest. *J Appl Physiol* 1976; 41: 659–667.
22. Eyles JG, Pimmel RL, Fullton JM, Bromberg PA. – Parameter estimates in a five-element respiratory mechanical model. *IEEE Trans Biomed Eng* 1982; BME-39, 460–463.
23. Ying Y, Peslin R, Duvivier C, Gallina C, Felicio da Silva J. – Respiratory input and transfer mechanical impedances in patients with chronic obstructive pulmonary disease. *Eur Respir J* 1990; 3: 1186–1192.
24. Jordan C, Lehane JR, Jones JG, Altman DG, Proyston JP. – Specific conductance using forced oscillation in mechanically ventilated human subjects. *J Appl Physiol: Respirat Environ Exercise Physiol* 1981; 51: 715–724.
25. Behrakis PK, Higgs BD, Baydur A, Zin WA, Milic-Emili J. – Respiratory mechanics during halothane anesthesia and anesthesia-paralysis in humans. *J Appl Physiol: Respirat Environ Exercise Physiol* 1983; 55: 1085–1092.
26. Chang HK, Mortola JP. – Fluid dynamic factors in tracheal pressure measurement. *J Appl Physiol: Respirat Environ Exercise Physiol* 1981; 51: 218–225.
27. Sullivan M, Paliotta J, Saklad M. – Endotracheal tube as a factor in measurement of respiratory mechanics. *J Appl Physiol* 1976; 41: 590–592.
28. Dixsaut G, Delavault E, Saumon G. – Impédance mécanique du système d'intubation des malades ventilés. *Bull Eur Physiopathol Respir* 1980; 16: 545–554.
29. Peslin R, Fredberg JJ. – Oscillation mechanics of the respiratory system. *In*: Macklem PT, Mead J, eds. Handbook of Physiology, Section 3, Vol. 3. Mechanics of Breathing, Part 1. Bethesda, Md, American Physiological Society, 1986; pp. 145–177.
30. Grimby G, Takishima T, Graham W, Macklem P, Mead J. – Frequency dependence of flow resistance in patients with obstructive lung disease. *J Clin Invest* 1968; 47: 1455–1965.
31. Michaelson ED, Grassman ED, Peters WR. – Pulmonary mechanics by spectral analysis of forced random noise. *J Clin Invest* 1975; 56: 1210–1230.
32. Nagels J, Landser FJ, van der Linden L, Clement J, van de Woestijne KP. – Mechanical properties of lungs and chest wall during spontaneous breathing. *J Appl Physiol: Respirat Environ Exercise Physiol* 1980; 49: 408–416.
33. Peslin R, Ying Y, Gallina C, Duvivier C. – Flow and volume dependence of forced oscillation resistance during quiet breathing in healthy subjects and in patients with chronic obstructive pulmonary disease (Abstract). *Eur Respir J* 1991; 4 (Suppl. 14): 462s.
34. Pimmel RL, Tsai MJ, Winter DC, Bromberg PA. – Estimating central and peripheral airway resistance. *J Appl Physiol: Respirat Environ Exercise Physiol* 1978; 45: 375–380.
35. Rotger M, Peslin R, Oostveen E, Gallina C. – Confidence intervals of respiratory mechanical properties derived from transfer impedance. *J Appl Physiol* 1991; 70: 2432–2438.
36. Lutchen KR, Jackson AC. – Reliability of parameter estimates from models applied to respiratory impedance data. *J Appl Physiol* 1987; 62: 403–413.
37. Rohrer R. – Der Strömungswiderstand in den menschlichen Atemwegen und der Einfluss der unregelmässigen Verzweigung des Bronchialsystems auf den Atmungsverlauf in verschiedenen Lungenbezirken. *Pfluegers Arch Gesamte Physiol Menschen Tiere* 1915; 162: 225–299.